



Fabrication of ZnO and TiO₂ Combined Activated Carbon Nanocomposite and Adsorption Enhanced Synergetic Photocatalytic Effects

LEI ZHU, SUN-BOK JO, SHU YE, KEFAYAT ULLAH and WON-CHUN OH*

Department of Advanced Materials Science & Engineering, Hanseo University, Chungnam 356-706, Republic of Korea

*Corresponding author: Fax: +82 41 6883352; Tel: +82 41 6601337; E-mail: wc_oh@hanseo.ac.kr

Received: 2 April 2013;

Accepted: 20 June 2013;

Published online: 10 March 2014;

AJC-14910

The ZnO-AC/TiO₂ compounds performance as photocatalyst have been investigated. The samples were checked by scanning electron microscopy, specific surface area, X-ray diffraction analysis and energy dispersive X-ray spectroscopy (EDX). The photocatalytic activities were evaluated by the photocatalytic oxidation of methylene orange solution. It was found that the prepared ZnO-AC/TiO₂ composite material having excellent photocatalytic activity under visible light irradiation. A small amount of ZnO in composites AC/TiO₂ significantly increase its photocatalytic activity.

Keywords: TiO₂, Activity carbon, Photocatalytic, Methylene orange.

INTRODUCTION

Industrial dyes including textile dyes are recognized as being an important environmental threat. It can be used for the treatment of such wastes physical, chemical and biological methods. The photocatalytic process using a TiO₂ photocatalyst is very promising for application to water purification, because many hazardous organic compounds can be decomposed and mineralized by the proceeding oxidation and reduction processes on the TiO₂ surface¹. Among the photocatalysts, TiO₂ has been most widely used because it is easily available inexpensive non-toxic and shows relatively high chemical stability²⁻⁵.

However, the main problem to be considered is shorter than 390 nm UV irradiation. TiO₂ photocatalytic activity, therefore, only a small portion (3-5 %) of the solar radiation can be used for degradation of environmental pollutants, because of their wide band gap. To widen the area of their practical application to indoor use, it has been considered that photocatalysts can be activated under visible light with yields would be indispensable⁶. TiO₂ having about 3.2 eV band gap, thus mainly the visible portion of the solar spectrum and only a small amount of ultraviolet absorption. Thus, for the high efficient photocatalytic activity it is necessary to extend the photo-response of TiO₂ to the visible spectrum by modification of its optical properties. Another problem is that the electrons and/or holes can be introduced for the electrical charge trap and thereby prolonging the reorganization time limit photoinduced electron-hole pairs high recombinant. Many methods have been proposed to solve these problems, but doping TiO₂ with

foreign ions is one of the most promising strategies for sensitizing TiO₂ to visible light and also for forming charge traps to keep electron-hole pairs separate⁷. The light of the titanium dioxide material in the visible range of the two methods have been applied to extend toward response shift: The one direction is a doped metal ions, anionic and synthetic from TiO₂ photocatalyst⁸⁻¹⁰, another is ion implantation¹¹⁻¹³. However, the ion implantation is quite expensive and possible only with high crystalline TiO₂. The doping of the metal element is a typical method, extended by providing titania spectrum in the band gap of the defect states in response to the visible light region¹⁴⁻¹⁶.

On the other hand, ZnO coated carbon nanotubes using filtered cathodic vacuum arc technology and modifications, as well as aligned ZnO nanowires by hydrothermal process on the carbon nanotube array growth has also been reported¹⁷⁻²¹. ZnO carries out this by increasing the charge separation and extending excitation energy range. Furthermore, the band gap energy of ZnO is much similar to that of TiO₂. Alternatively, ZnO is a main semiconductor for the synthesis of visible-light-active photocatalysts^{22,23}.

Several attempts have been adopted to enhance the photocatalytic performance of TiO₂, such as immobilization of TiO₂ powder onto supports like activated carbon fiber (ACF)²⁴ and activated carbon (AC). Activated carbon is highly adsorptive owing to its developed pore structure and high specific area. Moreover the particle size of commercially activated carbon is usually in the micro-scale range²⁵. Activated carbon was made an excellent alternative because it could concentrate

pollutants through adsorption around the loaded TiO₂, leading to an increase in the degradation of the pollutants²⁶.

In this study, activated carbon (AC) was treated by zinc oxide (ZnO) and TiO₂ to prepare ZnO-AC/TiO₂. X-ray diffraction was used to determine crystallinity. Scanning electron microscopy (SEM) was used to elucidate the mixing phenomenon and the size of ZnO-AC/TiO₂ composites. Energy dispersive X-ray (EDX) analysis was used to analyze the elements and their content in ZnO-AC/TiO₂ composites and a spectrophotometry was used to determine the decolorization of methylene orange solution which irradiation under visible light by different times.

EXPERIMENTAL

All chemical were used as received without further purification. Activated carbon was taken from coconut. The coconut shell was pre-carbonized first at 773 K and then activated by steam diluted with nitrogen in a cylindrical quartz tube at 1023 K for 0.5 h. This activated carbon was washed with deionized water and dried overnight in a vacuum drier at over 683 K. The titanium *n*-butoxide (TNB) as a titanium source was purchased from Kanto Chemical Company (TOKYO, Japan). Benzene was purchased as reagent-grade from Duksan Pure Chemical CO. (Korea). Titanium oxide nanopowder (TiO₂) with anatase structure used as control sample was purchased from Sigma-Aldrich Chemistry USA. Zn(NO₃)₂ was purchased from Duksan Pure Chemical CO. (Korea).

Preparation of ZnO-AC compounds: Active carbon was milled for 5 h, and treated with phosphoric acid. It was then dried at 373 K for 5 h, thus carbon powders were prepared. Carbon powder were mixed with 0.02 mol, 0.04 mol, 0.06 mol of Zn(NO₃)₂ solution, respectively. After stirring for 5 h and drying at 373 K, The mixture was heat treated at 773 K, finally the ZnO-AC compounds were formed.

Preparation of ZnO-AC/TiO₂ photocatalysts: The process of preparing ZnO-AC/TiO₂ photocatalysts used sol-gel method. A typical procedure is as follows: Due to fact that titanium *n*-butoxide is easily dissolved by benzene, 3 mL of titanium *n*-butoxide were added to 50 mL of benzene. The mixture was stirred for 5 h. TiO₂ and then support particles are first dried in the 323 K for 6 h and calcined at 773 K for each 2 h. ZnO-AC/TiO₂ (1) ZnO-AC/TiO₂ (2) ZnO-AC/TiO₂ (3) photocatalyst composites were obtained. The designations for different prepared materials are summarized in Table-1.

TABLE-1
NOMENCLATURE OF SAMPLES PREPARED

Preparation method	Nomenclatures
0.02 g ZnO-AC + 3 mL TNB + 50 mL C ₆ H ₆	ZnO-AC/TiO ₂ (1)
0.04 g ZnO-AC + 3 mL TNB + 50 mL C ₆ H ₆	ZnO-AC/TiO ₂ (2)
0.06 g ZnO-AC + 3 mL TNB + 50 mL C ₆ H ₆	ZnO-AC/TiO ₂ (3)

Characterization of prepared photocatalyst: Several techniques were used for the characterization of the ZnO-AC/TiO₂ composites. Crystalline phase, particle size and morphology of photocatalysts nanocrystals were investigated by specific surface area (BET), X-ray diffraction analysis, energy dispersive X-ray spectroscopy and scanning electron microscopy, respectively. The specific surface area (BET) was determined by N₂

adsorption measurements at 77 K. XRD analysis using radiation was performed to assess the crystalline phases. EDX spectra were used for the elemental analysis of the samples. SEM measurements were performed using a JEOL apparatus operating at 10 KV on specimens upon which a thin layer of gold or carbon had been evaporated. Determination of the photocatalytic activity of the catalyst is in the water solution of methylene orange decomposition. Photocatalytic quality 0.03 g was added to 50 mL of methylene orange solution concentration of 1.0 × 10⁻⁴ M, in the dark, until saturation adsorption of the mixture to invest at least 2 h. After adsorption, photodecomposition of the methylene orange solution to visible under light. Visible light (35 watts LED lamp) irradiated reactor for 0.5, 1.0, 1.5 and 2.0 h to complete, respectively, to study the degradation of methylene orange solution. The experiments were performed at room temperature.

RESULTS AND DISCUSSION

The nomenclatures of samples prepared are given in Table-1. The surface area was calculated using N₂ adsorption measurements at 77 K. As shown in Table-2, by increasing the introduction mass of ZnO units into the AC/TiO₂ structure *via* sol-gel procedure, the surface areas decreased. Usually the growth of TiO₂ crystallite and heat-treatment of the samples at 773 K caused the aggregation and sintering of the TiO₂ particles.

TABLE-2
EDX ELEMENTAL MICROANALYSIS
AND BET SURFACE AREA

Sample name	C (%)	O (%)	Zn	Ti (%)	BET (m ² /g)
ZnO-AC/TiO ₂ (1)	35.15	28.84	4.00	32.00	32.20
ZnO-AC/TiO ₂ (2)	40.68	29.84	6.01	23.47	51.24
ZnO-AC/TiO ₂ (3)	46.38	30.84	8.37	14.41	47.26

Fig. 1 showed the surface morphology by SEM at a magnification of 1000 times and 3000 times and surface of ZnO-AC/TiO₂ of compound and the ZnO catalyst and TiO₂ units. To the structure of ZnO-AC/TiO₂ units morphological evidence seems to cover the surface of the polymer. A uniform distribution of the units in the structure of the TiO₂ and ZnO-AC, continuous TiO₂ units is fixed at almost every one of the activated carbon (Fig. 1)²⁶. The EDX detector observation revealed the inclusive element of the prepared samples. Other elements like Ti and Zn were found in Fig. 2; may be these elements content in phosphoric acid. X-ray diffraction pattern is used to study the the phase structure of ZnO-AC/TiO₂ sample and shown in Fig. 3.

Fig. 3 shows the XRD patterns of the ZnO-AC/TiO₂ (1), ZnO-AC/TiO₂ (2) and ZnO-AC/TiO₂ (3) composites. It shows strong K α and K β peaks from Ti at 4.51 and 4.92 keV, whereas a moderate K α peak for O appears at 0.52 keV. After heat treatment at 773 K, major peaks were observed at 25.3, 37.9, 48.0, 53.8, 54.9 and 62.5° (2 θ), which were assigned to the (101), (004), (200), (105), (211) and (204) planes of anatase, indicating that the prepared TiO₂ is anatase. These results suggest that ZnO-AC/TiO₂ also has a pure anatase phase structure under the current preparation conditions. The XRD pattern shows peaks characteristics of ZnO. Additional ZnO

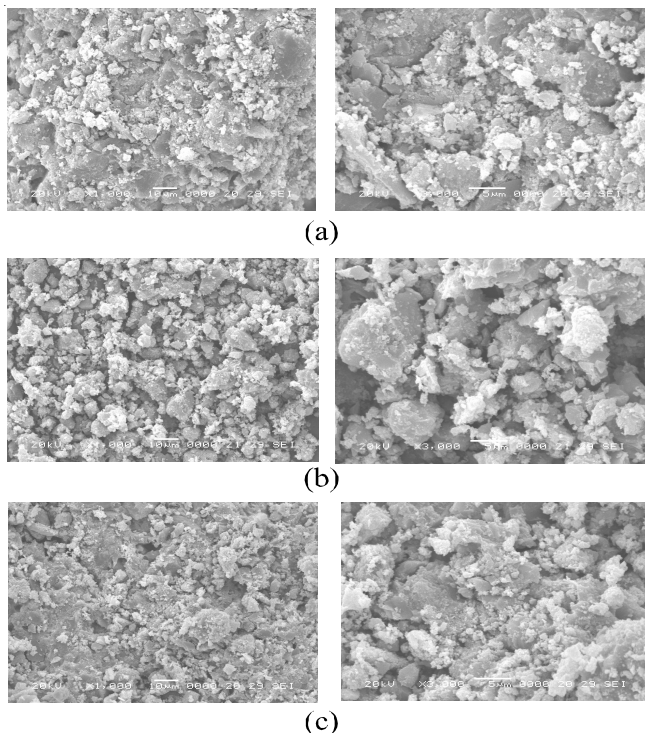


Fig. 1. SEM images of (a) ZnO-AC/TiO₂ (1) (b) ZnO-AC/TiO₂ (2) and (c) ZnO-AC/TiO₂ (3)

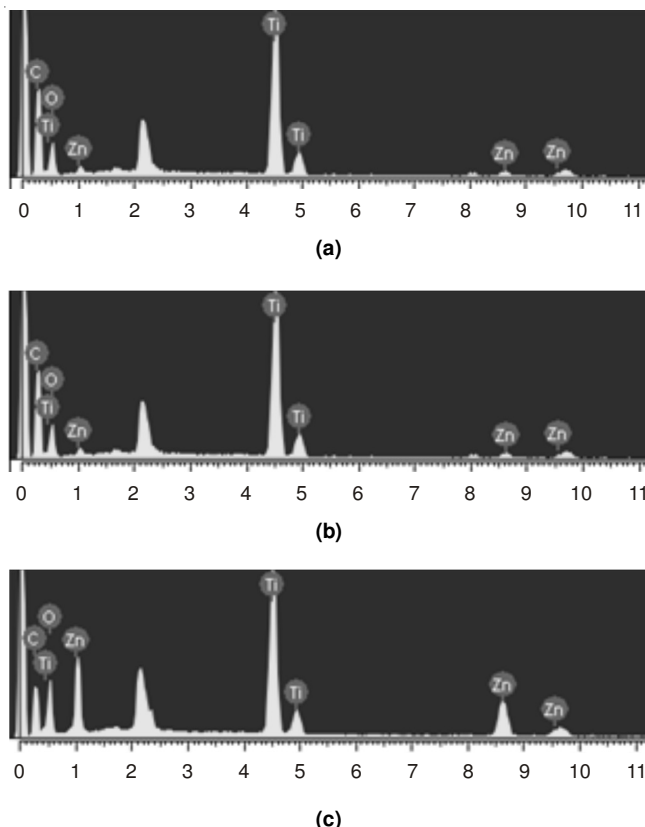


Fig. 2. EDX elemental microanalysis of photocatalysts, (a) ZnO-AC/TiO₂ (1), (b) ZnO-AC/TiO₂ (2) and (c) ZnO-AC/TiO₂ (3)

diffraction peaks for the (111) and (200) planes were observed²⁷ at 36.46 and 42.32° (2θ), respectively. All the diffraction characteristic peaks of the ZnO species in XRD can be readily assigned to the crystalline phase ZnO in a cubic structure. The

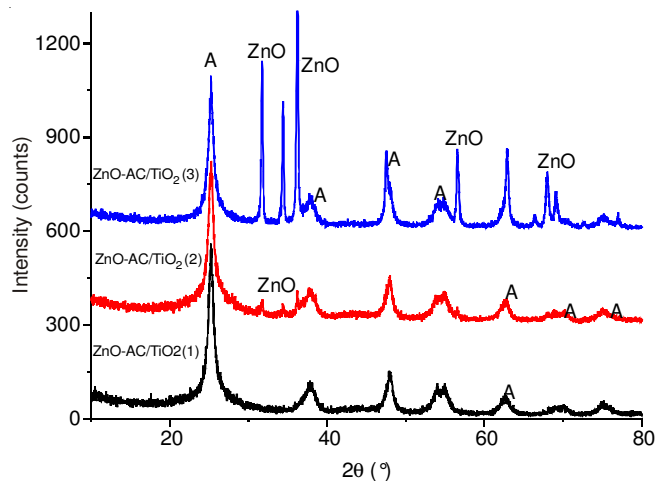


Fig. 3. XRD compounds of ZnO-AC/TiO₂(1), ZnO-AC/TiO₂ (2) and ZnO-AC/TiO₂ (3)

peaks of Zn were observed in the XRD pattern of the ZnO-AC/TiO₂ compound for the (111) and (200) planes at 43.33° and 50.64° (2θ). However, the peak intensity of ZnO was fairly weak. In the ZnO-AC/TiO₂ composite's XRD pattern, the intensity of the peaks concerning TiO₂ was decreased. This is because the TiO₂ content in the samples was decreased and this in turn influenced the ZnO peaks. For anatase and rutile structure of titania, as well as zinc, the characteristic diffraction peaks of the diffraction peak by X-ray diffraction (XRD) pattern check validation.

Fig. 4 shows the time series of methylene orange degradation using ZnO-AC/TiO₂ (1), ZnO-AC/TiO₂ (2) and ZnO-AC/TiO₂ (3) composites. In the adsorptive step, ZnO-AC/TiO₂ (1), ZnO-AC/TiO₂ (2) and ZnO-AC/TiO₂ (3) composites showed different adsorptive effects with AC-TiO₂ having the best adsorptive effect. In the degradation step, the ZnO-AC/TiO₂ (2) composites showed a good degradation effect. A comparison of the decoloration effect of the catalysts showed that ZnO-AC/TiO₂ (3) composites have best degradation effect²⁸⁻³⁰.

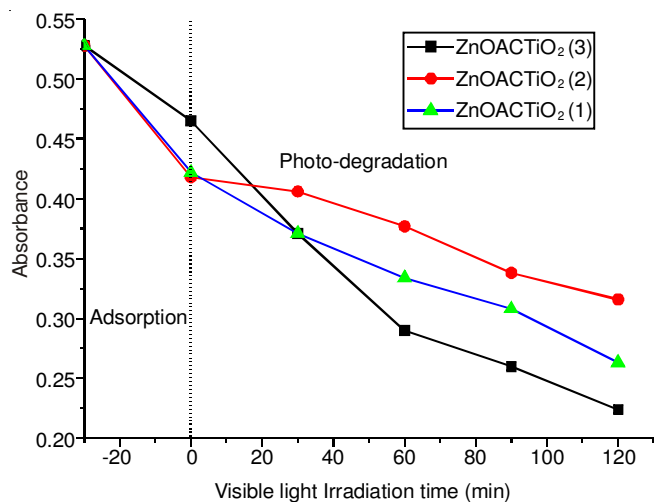


Fig. 4. Effect of photocatalyst amount on the methylene orange decolorization process in presence of ZnO-AC/TiO₂

Both the minimum conduction band and the maximum valence band of ZnO lie those of TiO₂; therefore the electrons

excited to the conduction band of the ZnO would transfer to the TiO₂, whereas the holes generated in the valence band in the TiO₂ prefer an opposing transfer to the ZnO. Charge carriers separated in different semiconductors effectively reduce the chance of electron-hole pair recombination and prolong their lifetime, thus increasing their quantum efficiencies. In addition, the working range of the wavelength is extended to a visible region due to absorption of visible light by ZnO, further enhancing the efficiency of the solar energy transition. Synergistic cooperation of these effects enables the ZnO/TiO₂ system to exhibit great potential for solar cell and photocatalysis applications. It is known that photocatalytic processes are based on electron hole pairs generated by means of band gap excitation. The photoinduced electron and hole could migrate to the surface to react with the adsorbed reactants in the desired process, or undergo an undesired recombination. Therefore, the generation and separation of the photoinduced electron hole pairs are the key factors to influence a photocatalytic reaction. In the photocatalytic process, TiO₂ semiconductor acts as a photocatalytic oxidation agent and a reductant. The generated electron-hole pairs in a photocatalytic process must be trapped in order to avoid recombination. The generated conduction band electrons (e⁻) probably reacted with dissolved oxygen molecules to yield superoxide radical anions O₂⁻, which on protonation generated the hydroperoxy HO₂ radicals, producing the hydroxyl radical OH, which was a strong oxidizing agent to decompose the organic dye²². Activated carbon has effective adsorbing properties and increases the surface area of the compounds which can increase the adsorption activity for samples, adsorbing more O₂ and dye molecules and ensuring these systems take full advantage of yield oxidizing species. The positive holes in the valence band can be trapped by OH⁻ or H₂O species adsorbed on the surface of the catalyst, producing reactive hydroxyl radicals in aqueous media. On the other hand, for commonly prepared ZnO nanopowders, especially in the range of 10-50 nm in diameter, they are easy to aggregate due to their large surface activity.

In present case, due to the reason that specific surface area obtained through BET approach includes the contribution of ZnO, it is difficult for us to quantitatively compare the samples' specific surface area. However, it can be seen from SEM images that ZnO nanopowders are uniformly dispersed on the surface. Since ZnO is the main contributor of the photocatalysis, ZnO with high dispersion is favorable to increase the reaction probability between catalysts and the adsorbed reactants, leading to a better photocatalytic property³¹. The degradation rate of pollutants are influenced by the active site and the photoabsorption of the catalyst used. Adequate loading of TiO₂/ZnO catalyst increases the generation rate of electron/hole pairs for enhancing the degradation of pollutants.

Conclusion

In this study, we present the preparation and characterization of ZnO and ZnO/TiO₂ composite photocatalysts synthesized by sol-gel method. SEM observation, activated carbon and ZnO on the surface of a composite material on the

titania particles embedded immobilized synthetic ZnO-AC/TiO₂ composite body. The XRD data shows ZnO-AC/TiO₂ composite material having a single crystal structure of anatase type. C and O and Ti and Zn was found from the EDX results. The methylene blue decomposition process confirmed the composite adsorption and photocatalytic reaction. ZnO-AC/TiO₂ samples showed strong absorption and effective decomposition of methylene orange solution under visible light. This was attributed to the three different effects between the photocatalytic reaction of the supported TiO₂, the energy transfer effects of ZnO, such as electrons and light and the separation effect in this system.

REFERENCES

1. M. Pera-Titus, V. García-Molina, M.A. Baños, J. Giménez and S. Esplugas, *Appl. Catal. B: Environ.*, **47**, 219 (2004).
2. M.L. Cheng and W.C. Oh, *Carbon Sci.*, **8**, 108 (2007).
3. W.-C. Oh, J.-H. Son, K. Zhang, Z.-D. Meng, F.-J. Zhang and M.-L. Chen, *J. Korean Ceram. Soc.*, **46**, 1 (2009).
4. W.C. Oh, A.R. Jung and W.B. Ko, *Mater. Sci. Eng. C*, **29**, 1338 (2009).
5. F.J. Zhang, J. Liu, M.L. Chen and W.C. Oh, *J. Korean Ceram. Soc.*, **46**, 263 (2009).
6. L. Zhu, Z.D. Meng, M.L. Chen, F.J. Zhang, J.G. Choi, J.Y. Park and W.C. Oh, *J. Photocatal. Sci.*, **1**, 69 (2010)
7. W.-C. Oh, F.-J. Zhang and M.-L. Chen, *J. Ind. Eng. Chem.*, **16**, 299 (2010).
8. W. Choi, A. Termin and M.R. Hoffmann, *J. Phys. Chem.*, **98**, 13669 (1994).
9. I. Justicia, P. Ordejon, G. Canto, J.L. Mozos, J. Fraxedas, G.A. Battiston, R. Gerbasí and A. Figueras, *Adv. Mater.*, **14**, 1399 (2002).
10. M. Anpo, Y. Yamashita and Y. Ichihashi, *Optronics*, **186**, 161 (1997).
11. R.G. Breckenridge and W.R. Hosler, *Phys. Rev.*, **91**, 793 (1953).
12. M. Anpo, *Pure. Appl.Chem.*, **72**, 1265 (2000).
13. H. Yamashita, M. Harada, J. Misaka, M. Takeuchi, Y. Ichihashi, F. Goto, M. Ishida, T. Sasaki and M. Anpo, *J. Synchrotron. Radiat.*, **8**, 569 (2001).
14. J.J. He, J.C. Zhao, T. Shen, H. Hidaka and N. Serpone, *J. Phys. Chem. B*, **101**, 9027 (1997).
15. J. Yu, J. Xiong, B. Cheng, Y. Yu and J. Wang, *J. Solid. State Chem.*, **178**, 1968 (2005).
16. X.H. Tang and D.Y. Li, *J. Phys. Chem. C*, **112**, 5405 (2008).
17. A. Matsumoto, K. Tsutsumi and K. Kaneko, *Langmuir*, **8**, 2515 (1992).
18. T. Hashishin, J. Murashita, A. Joyama and Y. Kaneko, *J. Ceram. Soc. Jpn.*, **106**, 1 (1998).
19. M. Inagaki, Y. Nakazawa, M. Hirano, Y. Kobayashi and M. Toyoda, *J. Inorg. Mater.*, **3**, 809 (2001).
20. A. Jitianu, T. Cacciaguerra, R. Benoit, S. Delpoux, F. Beguin and S. Bonnamy, *Carbon*, **42**, 1147 (2004).
21. L. Chen, B.L. Zhang, M.-Z. Qu and Z.-L. Yu, *Powder Technol.*, **1**, 154 (2005).
22. L. Huang, S.P. Lau, H.Y. Yang and S.F. Yu, *Nanotechnology*, **17**, 1564 (2006).
23. W.D. Zhang, *Nanotechnology*, **17**, 1036 (2006).
24. W.C. Oh and M.L. Chen, *J. Ceram. Process. Res.*, **9**, 100 (2008).
25. W.C. Oh, *J. Photocatal. Sci.*, **1**, 29 (2010).
26. J.G. Hou, Z. Wang, S.Q. Jiao and H.M. Zhu, *J. Hazard. Mater.*, **15**, 1772 (2011).
27. P.R. Ren, H.Q. Fan and X. Wang, *Catal. Commun.*, **25**, 32 (2012).
28. Z.D. Meng, K. Zhang and W.C. Oh, *J. Korean Ceram. Soc.*, **46**, 621 (2009).
29. C.H. Han, Z.Y. Li and J.Y. Shen, *J. Hazard. Mater.*, **168**, 215 (2009).
30. F.R. Xiu and F.S. Zhang, *J. Hazard. Mater.*, **172**, 1458 (2009).
31. X.D. Su, J.Z. Zhao, Y.L. Li, Y.C. Zhu, X.K. Ma, F. Sun and Z.C. Wang, *Colloids Surf. A*, **349**, 151 (2009).